FUDMA Journal of Engineering and Technology
ISSN: 3092-9385
https://fjet.fudutsinma.edu.ng/index.php/fjet/
Volume 2, Issue 1, 2026, 211-225

Development and Performance Evaluation of a Semi-Automated Impact Fracture Tester

Oluyemi S. ONIFADE[1*], Olusegun O. AJIDE[2]

[1*]Department of Welding and Fabrication Engineering Technology, Federal Polytechnic, Ilaro, Ogun State, Nigeria
[2]Department of Mechanical Engineering, University of Ibadan, Oyo State, Nigeria

[1*]sammyemmy_2020@yahoo.com, [2]ooe.ajide@gmail.com

Abstract

To evaluate the mechanical properties of metals and non-metals - such as tensile strength, compression, hardness, fatigue, flexural, and torsional strength - several standardized tests are used, and impact strength testing is essential for assessing the functionality, longevity, and safety of materials under abrupt loads. Izod impact testing, an ASTM standard method, is commonly used to assess the impact resistance of materials by measuring the energy absorbed during fracture. However, an affordable, locally manufactured substitute is required due to the high cost and unreliability of imported impact fracture testers. The design, construction, and testing of an Izod-based impact fracture tester created to examine the fracture properties of alloys under high strain rates are presented in this research. The machine consists of five primary components: a rigid frame, a pendulum hammer, a specimen clamp, a base, and a semi-automated digital display for data acquisition. After fabrication, the machine was tested and its performance evaluated by comparing its results with those from a standard testing machine. Three materials - Mild Steel, Aluminum, and High-Density Polyethylene (HDPE) - were selected to represent a spectrum of mechanical properties and fracture behaviors. Each specimen was machined to standard dimensions and tested in triplicate to ensure consistency. The primary evaluation metric was the energy absorbed until fracture, indicating the material's toughness. The fabricated machine demonstrated satisfactory performance, achieving a maximum energy of 58.41 J at a pendulum velocity of 3.9 m/s. The test results confirmed the effectiveness of the machine in assessing material toughness under high strain rates.

Keywords: *Pendulum, Izod impact test, Fracture, semi-automated, digital display.*

1.0 Introduction

Metallic materials are widely used by engineers in the design of structural and machine elements that are almost always subjected to external loadings and environmental conditions. Metallic materials fail in different modes depending on the type of loading (tensile, compressive, bending, shearing, or torsion) and on service conditions such as temperature and environmental corrosion.

Impact is a vital phenomenon that governs the service life of a structure. Taking an aircraft as an example, impact can occur due to bird strikes during cruising, take-off, or landing, as well as from debris present on the runway and other external factors. Impact loading must also be considered in road engineering where speed breakers exist, in bridge construction where moving vehicles induce dynamic loads, and in numerous other engineering applications. In studying the toughness of materials, impact tests are widely used. Material toughness refers to the ability of a material to absorb energy during plastic deformation, and this impact resistance is often temperature dependent.

Several researchers have emphasized the importance of impact testing in evaluating material performance under dynamic loading conditions. The foundational work of George R. Irwin introduced energy-based concepts of fracture, linking crack propagation to energy absorption [1]. Standard materials science literature highlights the importance of Charpy and Izod impact tests in determining ductile-to-brittle transition behaviour [2]. Furthermore, fracture toughness has been shown to be strongly influenced by strain rate and temperature, particularly in metallic alloys subjected to dynamic loading [3]. In aerospace applications, regulatory guidelines confirm that bird-strike and debris impacts significantly affect aircraft structural integrity, thereby necessitating reliable and standardized impact testing methods [4].

In engineering material development, fracture characteristics of metallic alloys are critical for safe and efficient design. However, the high cost of imported laboratory equipment has contributed to the shortage of fracture characterization facilities in many university laboratories, particularly in developing countries. Standard testing procedures specified by ASTM International often require sophisticated and expensive equipment [5]. Consequently, recent studies have focused on the development of cost-effective and locally fabricated testing machines to enhance experimental capabilities and promote technological self-reliance [6], [7]. These systems increasingly incorporate digital instrumentation, embedded sensors, and microcontroller-based data acquisition units to improve measurement accuracy and usability.

Received: 18/03/2026; Revised: 24/03/2026; Accepted: 26/03/2026; Published: 13/04/2026

As part of ongoing efforts to reduce dependence on foreign equipment and improve accessibility, there is a growing need to develop impact fracture testers capable of investigating the fracture characteristics of alloys under high strain rates. This need is particularly evident in developing regions, where limited access to standard testing facilities restricts experimental research, reduces hands-on training opportunities, and hinders innovation in material characterization.

Impact testing plays a crucial role in evaluating the toughness and fracture behaviour of engineering materials under sudden loading conditions. The ability of a material to absorb energy during fracture remains a key parameter in determining its reliability in structural and mechanical applications. The Izod impact test, standardized by International Organization for Standardization, is widely used for assessing the impact resistance of plastics and non-metallic materials under dynamic loading conditions [8]. Recent experimental investigations on instrumented Izod testing systems have demonstrated improved accuracy in measuring absorbed energy and fracture characteristics across materials with varying thicknesses and compositions [9].

Impact mechanics and the theoretical principles governing dynamic loading have been extensively studied. The fundamental principles of energy transfer during collisions emphasize the need for accurate and well-calibrated testing equipment [10]. Similarly, recent studies on high-strain-rate deformation behaviour have highlighted the significance of strain-rate sensitivity, material embrittlement, and dynamic fracture mechanisms under sudden loads [11]. These theoretical advancements provide a strong foundation for the design and optimization of modern impact testing systems.

The mechanics of pendulum motion, which forms the basis of many impact testing devices such as Izod and Charpy testers, has also been widely documented. The conversion of potential energy into kinetic energy during oscillation governs the impact energy delivered to the specimen, while gravitational effects influence the motion and repeatability of the pendulum system. These principles are essential in ensuring accurate energy measurement and system calibration in pendulum-type testing machines.

Recent research efforts have focused on the design and fabrication of specialized impact testing equipment for different materials and applications. Free-falling dart impact testers have been developed to evaluate the impact resistance of polymer films, with experimental results showing strong agreement with theoretical predictions [12]. Similarly, compact and digitally instrumented fracture testing machines have been developed as cost-effective alternatives to conventional universal testing systems, incorporating electronic control mechanisms and real-time data acquisition features [13].

Design improvements in impact testing machines have also been achieved through computational modelling and simulation techniques. Finite element analysis and three-dimensional modelling have been widely used to evaluate stress distribution, structural integrity, and energy transfer mechanisms in impact hammers and supporting structures, thereby enhancing system reliability and safety [14].

Standardized testing methods such as ASTM E23 and ISO 180 define specimen geometry, notch configuration, and testing procedures to ensure consistency and repeatability of impact testing results. These standards remain fundamental for ensuring comparability of experimental data across different laboratories and testing environments.

In addition to conventional pendulum-type testers, alternative impact testing systems have been developed to meet specific industrial requirements. Pneumatically operated impact testing machines have been utilized to investigate the dynamic behaviour of wooden and composite structures under controlled loading conditions [15]. Drop-weight impact testing machines have also been widely applied in automotive and structural engineering to evaluate material resistance to sudden impact loads [16].

Recent advancements in high-energy impact testing systems have enabled the simulation of extreme loading conditions such as rock bursts and ballistic impacts using hydraulic and high-velocity actuation mechanisms [17]. Furthermore, performance verification and calibration of impact testing machines remain critical, with studies demonstrating the influence of machine configuration, specimen geometry, and energy range on the accuracy of measured impact energy [18].

Impact testing is widely applied in evaluating the mechanical performance of engineering materials and structural components. Recent studies on welded mild steel joints have shown that welding parameters significantly influence impact toughness and energy absorption capacity [19]. Similarly, investigations on natural fibre-reinforced polymer composites have demonstrated the effectiveness of impact testing in assessing structural integrity and failure mechanisms [20].

Further research has explored the relationship between strain energy and absorbed impact energy using instrumented impact testing techniques, providing deeper insights into fracture behaviour under dynamic loading conditions [21].

Despite these advancements, many laboratories—particularly in developing regions—continue to face challenges related to the availability and cost of sophisticated testing equipment. Existing systems are often either fully manual or highly automated and expensive, creating a significant gap for affordable semi-automated testing

Received: 18/03/2026; Revised: 24/03/2026; Accepted: 26/03/2026; Published: 13/04/2026

machines that can provide reliable results while minimizing operational complexity [6], [7], [22]. This gap underscores the need for the development of cost-effective, accurate, and locally fabricated impact fracture testers.

Based on the reviewed literature, it is evident that several types of impact testing machines have been developed, including pendulum-type testers, drop-weight impact rigs, pneumatic testing machines, and hydraulic high-energy impact systems. However, there remains a need for cost-effective and locally fabricated systems capable of providing accurate and repeatable measurements while improving efficiency in laboratory testing. Therefore, the objectives of this study are to design a detailed apparatus and produce working diagrams of a locally developed impact testing device, to develop and fabricate a semi-automated impact fracture testing machine, and to conduct a performance assessment of the developed system using a case study involving impact fracture tests.

2.0 Methodology

The impact fracture testing machine was developed by leveraging available resources to design, fabricate, and assemble various components into a semi-automated testing device. The tester consists of five major components namely: a sturdy frame, a pendulum hammer, a clamping fixture for securing the specimen, and a digital display to read the data as shown in figure 1.

However, each component of the impact fracture tester was individually designed using Autodesk Inventor software and subsequently assembled into the final configuration. The fabricated parts were assembled and joined together using the permanent welding and temporary joining (bolts and nuts) in the workshop.

The impact fracture testing machine was developed by leveraging available resources to design, fabricate, and assemble various components into a semi-automated testing device. The tester consists of five major components namely: a sturdy frame, a pendulum hammer, and a clamping fixture for securing the specimen, and a digital display unit interfaced with an embedded sensing system comprising a load/force sensor mounted within the striker assembly. During impact, the sensor measures the transient force response and converts it into an electrical signal, which is subsequently conditioned through a signal processing circuit (amplification and filtering) and transmitted to a microcontroller-based unit that computes the absorbed impact energy based on calibrated relationships. The processed data are then relayed in real time to the digital display for direct readout of the energy absorbed, as shown in Figure 1. The design equations for the key components involved in the development and fabrication of the impact fracture tester, along with the corresponding dimensional calculations, are presented.

However, each component of the impact fracture tester was individually designed using Autodesk Inventor 2000 software and subsequently assembled into the final configuration. The fabricated parts were assembled and joined together using the permanent welding and temporary joining (bolts and nuts) in the workshop.

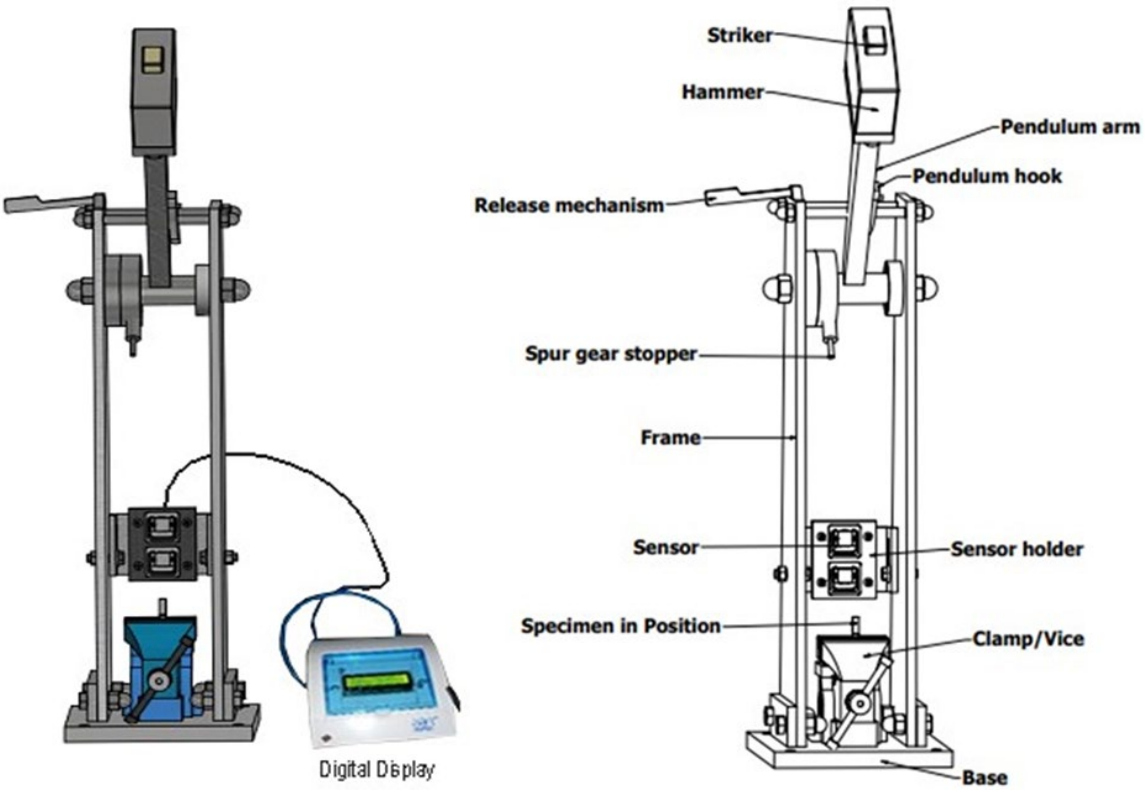

Figure 1: Major Parts of Impact Fracture Tester

Received: 18/03/2026; Revised: 24/03/2026; Accepted: 26/03/2026; Published: 13/04/2026

The clamp or fixture was mounted onto the base to which the frame was connected. The pendulum hammer was connected to the frame with a release mechanism. The pendulum hammer has an arm which must be rigid enough to clear specimens and reduce vibrations as in Figure 2. The head of the pendulum to strike the specimens was made of hardened steel, with a rectangular surface. The frame and pendulum were made rigid enough to maintain proper alignment of the hammer and specimen both in motion and at impact to reduce vibration and energy loss. (ASTM International, 2004).

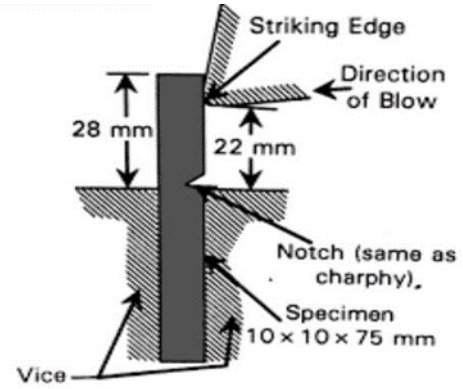

Figure 2: Impact Test Specimen in Position

2.1 Design of the Machine/Tester

The focus of this project is on the development and performance evaluation of (pendulum) impact fracture tester which will quantify the energy absorbed by a material.

The test involves measuring the energy rammed in breaking a notched specimen when hammered with the action of a swinging pendulum as shown in Figure 3.

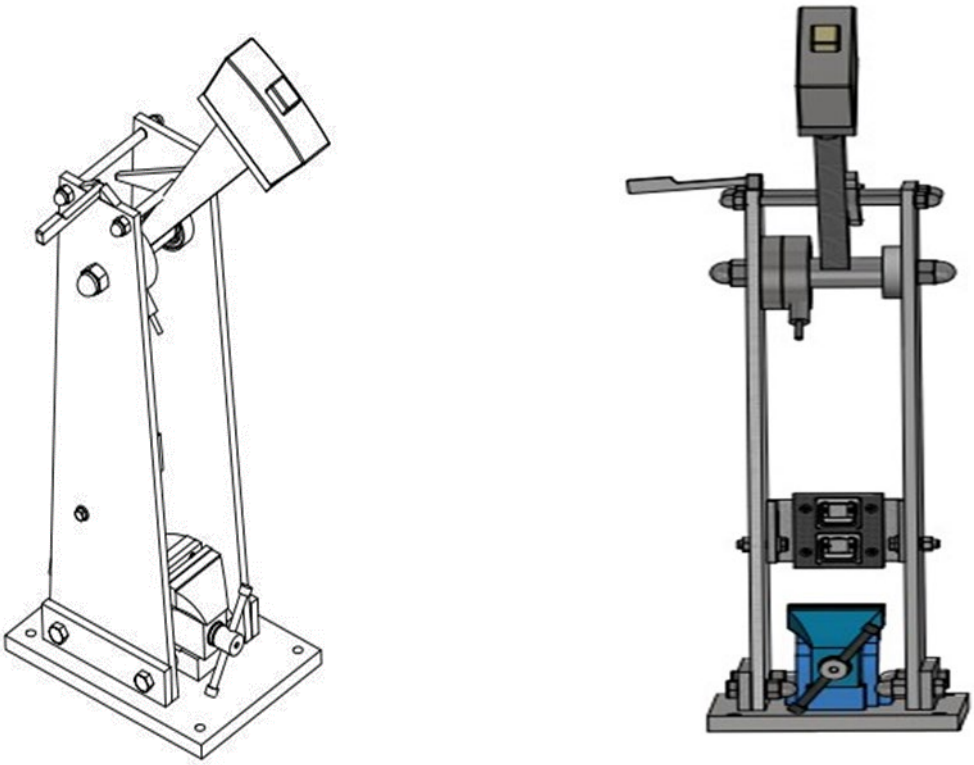

Figure 3: Schematic of Impact fracture tester

2.2 Design Equations for Major Parts of the Impact Fracture Tester

This section gives the design equations for major parts involved in the development and fabrication of the impact fracture tester. They are:

i. Shaft:

$$\frac{M}{I} = \frac{\sigma_b}{y} \quad (1)$$

Received: 18/03/2026; Revised: 24/03/2026; Accepted: 26/03/2026; Published: 13/04/2026

where M is the bending moment, I is the moment of inertia of cross-sectional area of the shaft about the axis of rotation, σ_b is the bending stress, and y is the distance from neutral axis to the outer-most fiber

For a round solid shaft, moment of inertia, $I = \frac{\pi}{64} \times d^4$ and $y = \frac{d}{2}$ (2)

Substituting these values in equation (2), to obtain

$$\frac{M}{z\frac{\pi}{64} \times d^4} = \frac{\sigma_b}{\frac{d}{2}}$$

Or $M = \frac{\pi}{32} \times \sigma_b \times d^3$ (3)

When the shaft is subjected to a bending load, the maximum stress (tensile or compressive) is given by the bending equation.

For a hollow shaft, the moment of inertia,

$$I = \frac{\pi}{64}[(d_0)^4 - (d_i)^4] = \frac{\pi}{64}((d_0)^4)(1 - k^4) \quad \left(\text{where, } k = \frac{d_i}{d_0}\right) \text{and } y = \frac{d_0}{2}$$

Again substituting these values in equation (3.1), we have

$$\frac{M}{\frac{\pi}{64}((d_0)^4)(1-k^4)} = \frac{\sigma_b}{\frac{d_0}{2}} \qquad or\ M = \frac{\pi}{32} \times \sigma_b \times (d_0)^3\,(1 - k^4) \tag{4}$$

where d_0 is the outside diameter of the hollow shaft and d_i is the inner diameter of the hollow shaft

From this equation, the outside diameter of the shaft (d_0) may be obtained

ii. **Flat Plate (Base)**

Since the base plate carries the weight of all other components of the impact fracture tester such as pendulum, clamp, etc., it will be subjected to bending stress as given in the relation below:

$$\sigma_b = \frac{My}{I} \tag{5}$$

where M is the bending moment acting at the given section, σ_b is the bending stress, I is the moment of inertia of the cross-section about the neutral axis, and y is the distance from the neutral axis

Bending stress at the edge of a hole for transverse bending of such plate is given by relationship:

$$\sigma_b = \frac{My}{I} = \frac{6M}{(b-d)t^2} \tag{6}$$

For four holes, the stress will be $\sigma_b = \frac{My}{I} = \frac{6M}{4(b-d)t^2}$ (7)

where M is bending moment at the edges of plate, b is plate width, d is the hole diameter, t is the plate thickness

iii. **Frame**:

The frame (Trapezoidal in shape) is the part that supports and suspends the pendulum, and there is tendency for it to experience bending which can be obtained with the expression below:

$$\sigma_b = \frac{My}{I} \tag{8}$$

For the Trapezoidal face, Area, $A = \frac{h}{2}(b + a)$; Centroid $\bar{y} = \frac{h}{3}\frac{(b+2a)}{(b+a)}$ (9)

Parallel axis theorem state that: $I = \bar{I}_x + Ad_y^{\,2}$ (10)

iv. Round bar:

A stud is a round bar threaded at both ends. One end of the stud is screwed into a tapped hole of the parts to be fastened, while the other end receives a nut on it. Studs are chiefly used instead of tap bolts for securing various kinds of covers e.g. covers of engine and pump cylinders, valves, chests etc.

The studs usually carry a load in the direction of the stud axis which induces a tensile stress in the stud.

Let $d_c = Root\ or\ core\ diameter\ of\ the\ thread$

$\sigma_t = permissible\ tensile\ stress\ for\ the\ stud\ material$

The external load applied, $F = \frac{\pi}{4}(d_c)^2\sigma_t$ (11)

Or $d_c = \sqrt{\frac{4F}{\pi\sigma_t}}$ (12)

v. Fastener:

The purpose of the bolt as fastener is to clamp two or more parts together. Twisting the nut stretches the bolt to produce the clamping force. This clamping force is called the pre-tension or bolt preload. It exists in the connection after the nut has been properly tightened no matter whether the external tensile load P is exerted or not. Of course, since the members are being clamped together, the clamping force that produces tension in the bolt induces compression in the members.

Since all the joint tend to experience shear,

$$\tau = \frac{Force}{Area} = \frac{F}{A} \tag{13}$$

Received: 18/03/2026; Revised: 24/03/2026; Accepted: 26/03/2026; Published: 13/04/2026

where $A = \frac{\pi d^2}{4}$ (14)

Also considering the yield strength and factor of safety, the equation becomes:

$$\tau = \frac{F}{\frac{\pi d^2}{4}} = \frac{Syp}{2n} \quad (15)$$

$$4 \times F \times 2 \times n = \pi \times Syp \times d^2$$

$$d^2 = \frac{4 \times F \times 2 \times n}{Syp \times \pi} \quad (16)$$

vi. Pendulum arm

$$\sigma_b = \frac{My}{I} \quad (17)$$

To determine the centroid of the pendulum arm, the following equations are used.

Hollow circle: Area, $A = \frac{1}{2}\pi({r_0}^2 - {r_i}^2)$; Centroid: $\bar{y} = \frac{\pi {D_o}^4}{64} - \frac{\pi {D_i}^4}{64}$; (18)

Trapezoidal part: Area, $A = \frac{h}{2}(b + a)$ Centroid: $\bar{y} = \frac{h}{3}\frac{(b+2a)}{(b+a)}$ (19)

Rectangular part: Area, $A = bh$ Centroid: $\bar{y} = \frac{h}{2}$ (20)

To find the moment of inertia of the arm the following equations are considered

For hollow circle, $I_x = \frac{1}{2}(A)({r_0}^2 + {r_i}^2)$ where, $A = \pi({r_0}^2 - {r_i}^2)$ (21)

For trapezoidal face. $I_x = \frac{h^2}{36}\frac{(a^2+4ab+b^2)}{(a+b)}$ (22)

For rectangular face, $I_x = \frac{bh^3}{12}$ (23)

The parallel-axis theorem gives the relationship between the moment of inertia with respect to a centroid axis and the moment of inertia with respect to any parallel axis.

$$I_x = \bar{I_x} + A{d_y}^2 \quad (23)$$

vii. Bearing Selection and Bearing Design:

The approximate rating (or service) life of ball or roller bearings is based on the fundamental equation,

$$L_{10} = \left(\frac{C}{P}\right)^p \quad (24)$$

$$C = P(L_{10})^{1/p} \text{ Or } \frac{C}{P} = {L_{10}}^{\frac{1}{p}} \quad (25)$$

where L_{10} is basic rating life in millions of revolutions, C is equivalent of basic dynamic loading rating (N), P is equivalent dynamic bearing load, P is exponent for the life equation (P for ball bearing is $\frac{1}{3}$ and P for roller bearing is $\frac{10}{3}$)

The related values of load ratio $\frac{C}{P}$ and L_{10} are set in the life calculation chart in Appendix IV

For bearing operating at constant speed, it may be more convenient to deal with basic rating life expressed in operating hours using: $L_{10h} = \frac{1000000}{60N}\left(\frac{C}{P}\right)^p$ (26)

where L_{10h} is the basic rating life in operating hours, and N is the rotational speed r/min.

Oscillating loads: When a bearing does not make a complete rotation but back and forth in operation, a lower equivalent radial load can be calculated using the formula below:

$$P = P_0 \times \left(\frac{\beta}{90}\right)^{1/p} \quad (27)$$

Where P is equivalent dynamic radial load, P_o is the actual oscillating radial load, and β is the angle of oscillation in degrees $p = \frac{10}{3}$ (Roller Bearings)

$p = \frac{1}{3}$ (Ball Bearings)

2.3 Design of Machine

The mild steel base with dimensions of 320 mm × 225 mm × 20 mm was chosen to support the whole structure. The pendulum was chosen as a trapezoidal shaped as shown in Figure 4. The pendulum was constructed from 25 mm thick trapezoidal mild steel bar with a length of 447 mm from the center of swing. The total mass of the pendulum arm hammer is 7.683 kg.

Received: 18/03/2026; Revised: 24/03/2026; Accepted: 26/03/2026; Published: 13/04/2026

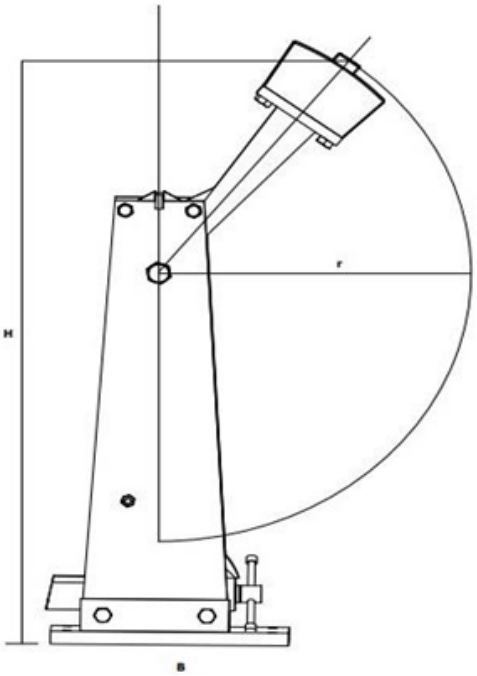

Figure 4: Maximum angle and energy stored in the position

The maximum angle the pendulum can swing is 150° with vertical and the maximum energy stored in this position

$$= mgh1$$
$$= 7.683 \times 9.81 \times 0.415 \times (1 - cos150°)\ Nm$$
$$= 58.41\ J$$

Thus, the maximum velocity achieved,

$$V = \sqrt{2gh_1}. \quad (28)$$
$$= \sqrt{2}\times 9.81 \times 0.415 \times (1 - cos\ 150°)$$
$$= 3.9\ m/s$$

After calculation of various parameters, the specification of the designed impact fracture tester is as follows and is shown in Figure 5. The clamp was purchased from the local market.

2.3.1 Machine Specification:

Base dimension = 320 mm× 225mm × 20 mm
Clamp dimension = 100mm ×80 × 70.98mm
Pendulum cross-section = 90 mm × 10.27 mm
Pendulum mass, m = 8 kg
Pendulum radius, r = 366mm
Range of pendulum swing angle = 0° to 150°
Tolerance angle or error angle = 2°
Striking velocity of pendulum= 3.9 m/s

Received: 18/03/2026; Revised: 24/03/2026; Accepted: 26/03/2026; Published: 13/04/2026

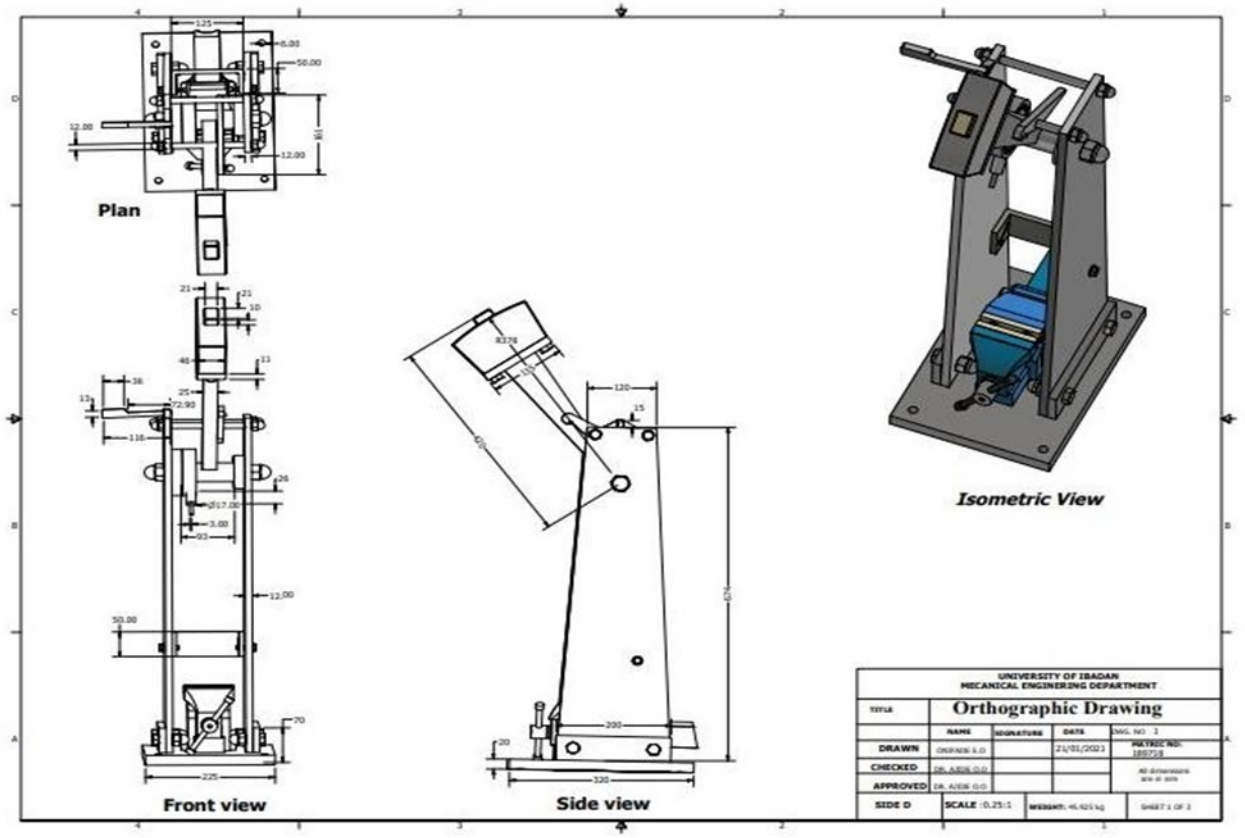

Figure 5: Orthographic views of Impact Fracture Tester

2.4 Design Expressions for the Impact Fracture Tester

1. Torque Analysis of the Pendulum Shaft

The pendulum motion induces torque about the pivot shaft, which can be expressed as:

$$T = F \times r \tag{29}$$

For a pendulum system, the torque acting on the shaft is given by:

$$T = mgLsin\theta \tag{30}$$

where T is the torque (N·m), m is the mass of the pendulum hammer (kg), g is the acceleration due to gravity (9.81 m/s²), L is the distance from the pivot to the center of mass of the pendulum (m) and θ is the angular displacement (rad)

This expression is critical in sizing the shaft diameter to withstand torsional loading without failure.

2. Impact Energy and Energy Absorption

The energy available at impact is derived from the potential energy of the raised pendulum:

$$E = mg(h_1 - h_2) \tag{31}$$

where E is the impact energy absorbed by the specimen (J), h_1 is the initial height of the pendulum (m) and h_2 is the final height after fracture (m)

Alternatively, the kinetic energy at the point of impact is:

$$E = \frac{1}{2}mv^2 \tag{32}$$

where v is velocity of the pendulum at impact (m/s)

These relations form the basis for evaluating the energy absorbed during fracture of the test specimen.

3. Fatigue Strength of Structural Components

The structural members of the tester (frame, shaft, and supports) are subjected to cyclic loading during repeated testing. Fatigue strength can be estimated using the stress-life relationship:

$$\sigma_a = \sigma`_f (2N)^b \tag{33}$$

where σ_a is the alternating stress (MPa), $\sigma`_f$ is the fatigue strength coefficient, N is the number of cycles to failure, and b is the fatigue strength exponent

For safe design under repeated loading:

$$\sigma_{max} \leq \frac{\sigma_y}{FS} \tag{34}$$

where σ_y is the yield strength of the material and FS is the factor of safety

This ensures that the structural components can withstand repeated impact operations without failure.

Received: 18/03/2026; Revised: 24/03/2026; Accepted: 26/03/2026; Published: 13/04/2026

4. Structural Strength of the Frame and Support Members

The frame and supporting columns must resist bending and shear stresses induced by the pendulum impact and machine weight.

Bending stress is given by: $$\sigma = \frac{My}{I} \quad (35)$$

Where σ is the bending stress (Pa), M is the bending moment (N·m), y is the distance from the neutral axis (m) and I is the second moment of area (m^4)

Shear stress is given by:

$$\tau = \frac{VQ}{It} \quad (36)$$

Where τ is the shear stress (Pa), V is the shear force (N), Q is the first moment of area (m^3), t is the thickness of the section (m)

These expressions are essential in determining appropriate material selection and cross-sectional dimensions for the structural frame shown in the orthographic drawing.

5. Design Implication

The integration of torque, impact energy, fatigue, and structural strength analyses ensures that the tester is mechanically stable, safe, and capable of delivering repeatable and reliable results. These expressions guided the selection of the shaft diameter, frame thickness, pivot design, and overall structural configuration of the fabricated machine.

3.0 Results and Discussion

3.1 Experimental Procedure

There are several standards for impact test. The ASTM standard for Izod Impact test for metals is ASTM E23 – Notched Bar Impact Test of Metallic Materials. ASTM E23 outlines the procedures for Charpy (simple beam) and Izod (cantilever beam) notched-bar impact testing of metallic materials, aimed at determining the energy absorbed during fracture. The result is expressed as energy lost per unit thickness (say, J/cm) at the notch. The dimension of a standard specimen for ASTM E23 is 75 mm × 10 mm × 10 mm. The test specimen varies on which material is being tested. The specimen is held at one end and the other end is free. A 45° V-notch of depth 2 mm is cut at the middle. The experimental setup depends on the setting up of the specimen on the clamp and the angle of the pendulum where it is freed. These are: (i) Setup on the clamp and (ii) Angle graduation.

3.1.1 Setup on the Clamp:

The specimen is set on the clamp tightly and rigidly. The middle section of the V-notch is situated at the midpoint of the clamp. As illustrated in Figure 6, the pendulum striking edge must impact the specimen at a point 22 mm above the clamp.

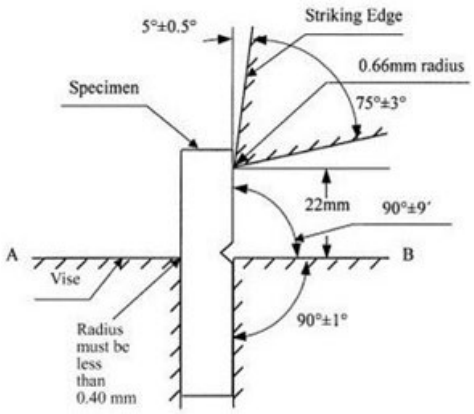

Figure 6: Striking Edge and Striking Position (Kobayashi)

Angle graduation: First of all, from an assumable angle, the pendulum is swung and then decreases it gradually onto the angle where the fracture actually occurred. The digital display connected to the sensor indicates the amount of energy absorbed by the specimen. Figure 7 illustrates the machine in three-dimensional form, while Figures 8–10 present photographic views of the experimental setup

Received: 18/03/2026; Revised: 24/03/2026; Accepted: 26/03/2026; Published: 13/04/2026

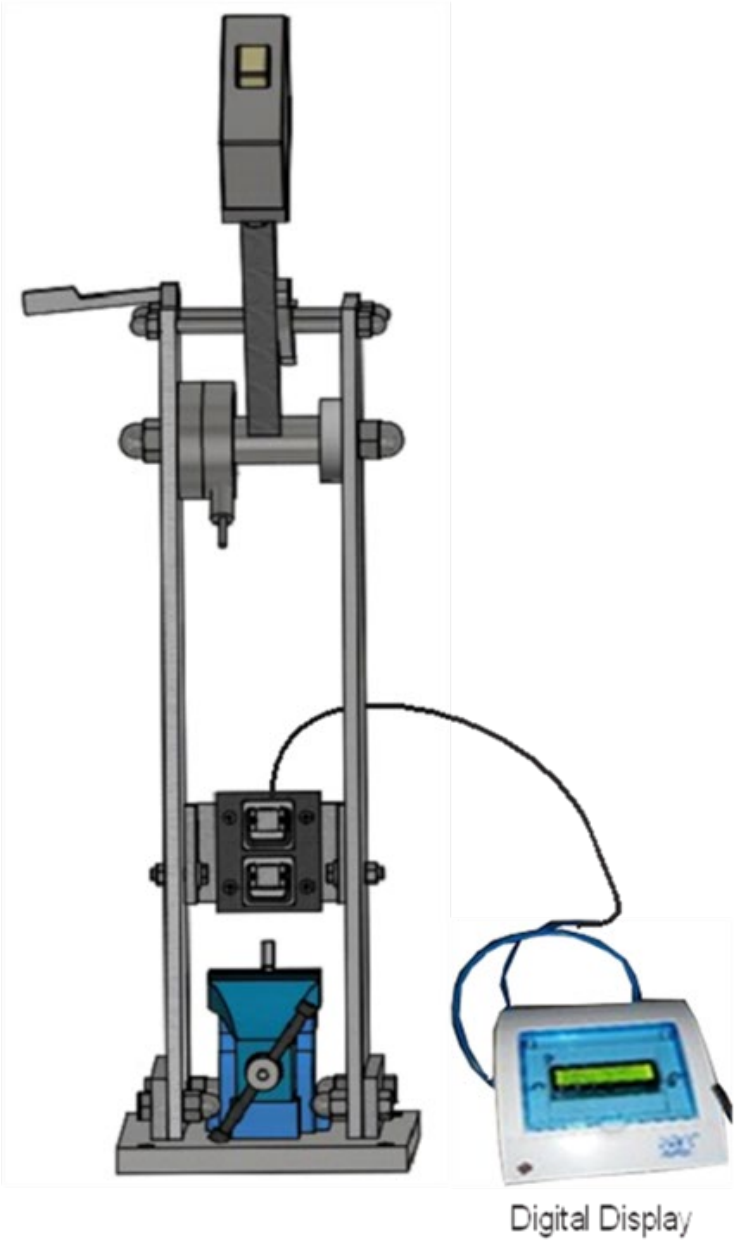

Figure 7: Impact fracture tester experimental set- up in 3-D

Received: 18/03/2026; Revised: 24/03/2026; Accepted: 26/03/2026; Published: 13/04/2026

Figure 8: Impact fracture tester experimental set- up

Figure 9: Photo of Experimental setup from Front

Figure 10: Photo of Experimental setup from Top

Received: 18/03/2026; Revised: 24/03/2026; Accepted: 26/03/2026; Published: 13/04/2026

3.2 Performance Test

The performance test was carried out with the constructed Impact Fracture tester in which three different specimen samples of different materials —Mild Steel, Aluminum, and High-Density Polyethylene (HDPE)—were tested on both the newly constructed Impact Fracture Tester (IFT) and a standard impact testing machine. The data include individual trial measurements as well as summary averages and percentage differences to compare the two testing methods.

3.2.1 Experimental Setup

Specimens: Three replicates for each material.
Testing Machines:
Impact Fracture Tester (IFT): The newly developed apparatus.
Standard Impact Testing Machine (SM): A widely accepted machine used as a benchmark.
Measured Parameter: Energy absorbed (in Joules) during fracture.
Testing Conditions: All tests were performed under standard laboratory conditions with identical specimen orientations and striking conditions for both machines.

3.3 Experimental Data

3.3.1 Individual Trial Data

The table 1 below shows the energy absorption values (in Joules) recorded for each trial on both the IFT and the standard machine.

As shown in Figure 11, the energy absorption values obtained from the Impact Fracture Tester closely follow the trend observed with the standard machine across all trials and materials.

Table 1: The energy absorption values (in Joules)

S/N	Specimen Material	Trial	Impact Fracture Tester (IFT) Energy (J)	Standard Machine (SM) Energy (J)
1	Mild Steel	1	258	263
		2	255	260
		3	260	264
2	Aluminum	1	125	127
		2	123	125
		3	126	128
3	HDPE	1	95	98
		2	93	96
		3	94	99

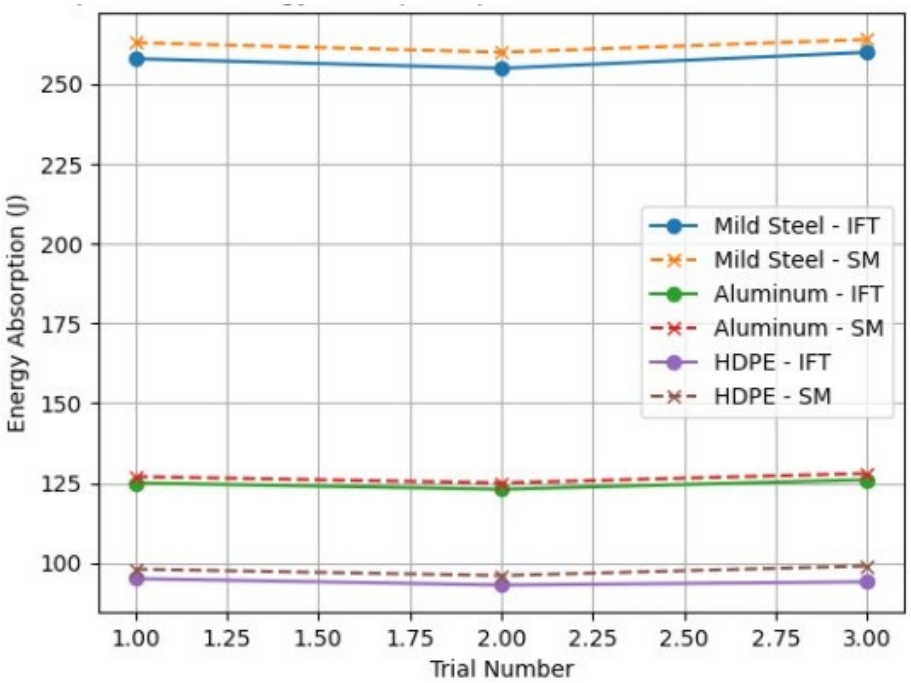

Figure 11: Comparison of energy absorption values (J) obtained from the Impact Fracture Tester (IFT) and the Standard Machine (SM) across three trials for Mild Steel, Aluminum, and HDPE.

Received: 18/03/2026; Revised: 24/03/2026; Accepted: 26/03/2026; Published: 13/04/2026

3.4 Summary Data and Comparative Analysis

Averages and percentage differences between the two testing devices were computed as follows:

Averaging:

For each material, the average energy absorbed was calculated over the three trials as shown in Table 2

Percentage Difference:

$$\%Difference = \frac{\text{Avg. SM} - \text{Avg. IFT}}{\text{Avg. SM}} \times 100\% \quad (37)$$

Figure 12 illustrates that the average energy values for both testing methods are in close agreement, with percentage differences below 4%, thereby confirming the reliability and accuracy of the developed tester.

Table 2: Summary Data and Comparative Analysis of Energy Absorption

Specimen Material	Average IFT Energy (J)	Average Standard Energy (J)	% Difference
Mild Steel	257.7	262.3	1.76%
Aluminum	124.7	126.7	1.58%
HDPE	94.0	97.7	3.79%

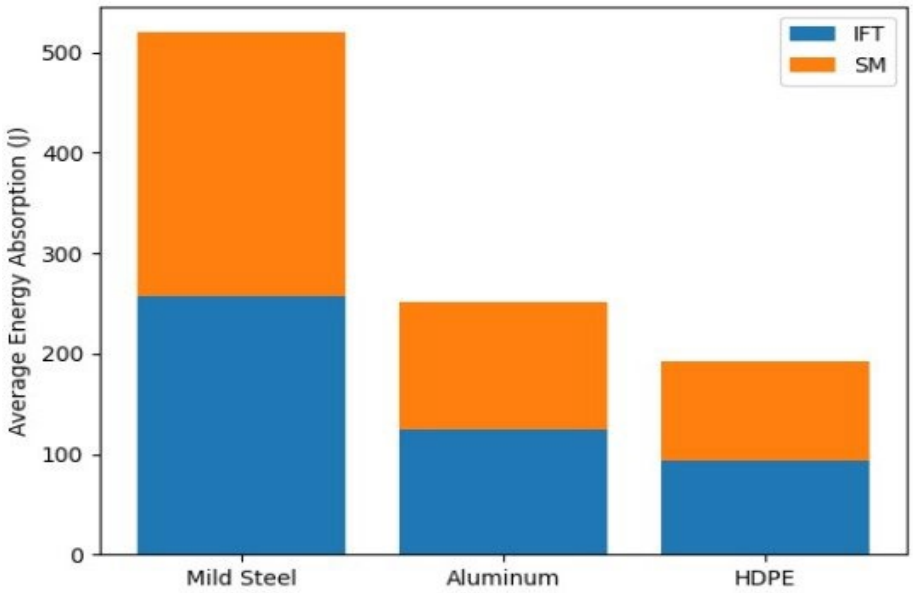

Figure 12: Average Energy Absorption Comparison

3.5 Discussion

The experimental results obtained from the developed Impact Fracture Tester (IFT) show strong agreement with those from the standard impact testing machine across all tested materials. This confirms the reliability and practical applicability of the constructed device for evaluating impact energy absorption under controlled conditions.

For mild steel, the highest energy values were recorded, consistent with its ductile nature and high toughness. The small percentage difference of approximately 1.76% indicates that the developed tester accurately captures the fracture behaviour of high-strength metallic materials. The consistency across repeated trials also demonstrates good repeatability and stability, reflecting effective mechanical alignment and proper functioning of the pendulum and measurement system.

In the case of aluminum, which exhibits moderate toughness, the results similarly show close agreement between both testing systems, with a percentage difference of about 1.58%. This confirms that the tester maintains accuracy for materials with intermediate mechanical properties and is sufficiently sensitive to variations in energy absorption.

For high-density polyethylene (HDPE), a relatively higher variation of approximately 3.79% was observed, though still within acceptable experimental limits. This can be attributed to the viscoelastic behaviour of polymeric materials, which are more sensitive to strain rate, temperature, and specimen preparation. Despite this, the results remain sufficiently close, validating the tester's applicability to polymer materials.

3.6 Comparative Discussion with Existing Studies

The performance of the developed IFT is consistent with findings reported in recent studies. The observed deviations (below 4%) align with results by Patel *et al.* [6], who reported differences within 5% for a semi-

Received: 18/03/2026; Revised: 24/03/2026; Accepted: 26/03/2026; Published: 13/04/2026

automated impact testing system, confirming that locally fabricated machines can achieve reliable accuracy when properly designed.

Similarly, the consistency in measurements agrees with the work of Rahman and Islam [7], where digital instrumentation improved accuracy and repeatability. The integration of a sensor-based system in the present study contributes to reduced human error and enhanced measurement precision.

For metallic materials, the results follow trends reported by Saluja *et al.* [19], indicating that impact energy measurements remain consistent across calibrated systems despite variations in material properties. For polymeric materials, the slightly higher variation observed for HDPE agrees with Appusamy *et al.* [20], who reported increased variability due to the viscoelastic nature of such materials.

The slight underestimation of absorbed energy observed in this study is also consistent with findings by Kumar and Singh [9], where minor energy losses due to friction, air resistance, and alignment were identified as common sources of deviation in fabricated systems.

Overall, the developed tester shows a slight but consistent underestimation of absorbed energy compared to the standard machine. This deviation is minimal and can be attributed to mechanical losses and minor alignment differences, which are typical in newly developed testing equipment and can be reduced through further calibration and design refinement.

The low percentage differences (all below 4%) and consistent repeatability demonstrate that the tester meets acceptable engineering accuracy for laboratory-scale applications. This makes it suitable for both educational and research purposes, particularly in environments where access to standard testing machines is limited.

In summary, the developed Impact Fracture Tester demonstrates reliable performance in measuring impact energy across both metallic and polymeric materials. Its close agreement with standard machine results and consistent repeatability confirm its effectiveness as a cost-effective alternative for impact testing. Future improvements should focus on minimizing systematic losses and enhancing measurement precision, especially for materials with highly variable fracture behaviour.

3.7 Conclusion

The performance evaluation results indicate that the fabricated Impact Fracture Tester provides energy absorption measurements that are comparable to those obtained from a standard impact testing machine. For all materials tested, the observed percentage differences remained below 4%, demonstrating a high level of agreement, and thereby confirming the reliability and accuracy of the developed system. The maximum energy recorded was 58.41 J at a pendulum velocity of 3.9 m/s, indicating the machine's capability to effectively evaluate the fracture characteristics of metallic specimens under dynamic loading conditions.

The results further show that the developed tester can be effectively utilized for assessing the impact resistance of metals of varying thicknesses, making it suitable for use in materials and applied mechanics laboratories. Its successful fabrication and performance validation demonstrate the feasibility of locally developing cost-effective alternatives to imported impact testing equipment. In addition, the availability of such a system enhances experimental learning by providing students with practical exposure to fracture behaviour under impact loading.

3.8 Recommendation

Regular calibration of the impact fracture tester is recommended to maintain measurement accuracy, particularly when changes in hammer size or mass are introduced. Although the fabrication process proved economical compared to procuring a commercial machine, continued attention should be given to safety measures to ensure safe operation for users and observers. Future improvements may focus on extending testing to a wider range of materials and environmental conditions, as well as upgrading the system from semi-automated to fully automated operation to enhance precision, repeatability, and user convenience.

Acknowledgement

The authors would like to express their sincere gratitude to the technical staff and academic advisors in the Department of Mechanical Engineering, Faculty of Technology, University of Ibadan, for their support during the design, fabrication, and evaluation stages of this project.

References

[1] George R. Irwin, "Analysis of stresses and strains near the end of a crack traversing a plate," *J. Appl. Mech.*, vol. 24, pp. 361–364, 1957.
[2] Materials Science and Engineering: An Introduction. New York, NY, USA: Wiley, 2014.
[3] Mechanical Metallurgy. New York, NY, USA: McGraw-Hill, 1986.
[4] Federal Aviation Administration, *Aircraft Certification: Bird Strike Requirements*, Washington, DC, USA, 2018.
[5] ASTM International, *Standard Test Methods for Notched Bar Impact Testing of Metallic Materials (ASTM E23)*, West Conshohocken, PA, USA, 2018.

[6] J. Patel, R. Shah, and M. Desai, "Development of a semi-automated impact testing machine with digital energy measurement," *Int. J. Mech. Prod. Eng. Res. Dev.*, vol. 10, no. 3, pp. 733–740, 2020.
[7] M. Rahman and M. Islam, "IoT-based smart impact testing machine for real-time monitoring and data logging," *IEEE Access*, vol. 9, pp. 118345–118353, 2021.
[8] International Organization for Standardization, *Plastics—Determination of Izod Impact Strength (ISO 180)*, Geneva, Switzerland, 2019.
[9] R. Kumar and P. Singh, "Design of a digitally instrumented Charpy impact testing machine with strain gauge measurement," *Measurement*, vol. 162, p. 107114, 2020.
[10] Impact Mechanics. Cambridge, U.K.: Cambridge Univ. Press, 2000.
[11] Y. Yang and Z. Zhang, "High strain-rate fracture behaviour of engineering materials under impact loading," *Mater. Sci. Eng. A*, vol. 772, p. 138146, 2020.
[12] M. Musaddique, A. Hussain, and S. Ahmed, "Free-falling dart impact testing method for toughness evaluation of polymer films," *Polymer Testing*, vol. 92, p. 106115, 2021.
[13] R. Kumar and S. Singh, "Design and fabrication of a compact fracture toughness testing machine," *Int. J. Mech. Eng. Technol.*, vol. 9, no. 5, pp. 120–128, 2018.
[14] L. Chen, H. Sun, and Y. Wu, "Structural optimization of pendulum impact testing machines using numerical simulation," *Eng. Struct.*, vol. 215, p. 110118, 2020.
[15] S. Ughade, R. Patil, and A. Deshmukh, "Development of a pneumatically operated impact testing machine for wooden structural components," *Int. J. Mech. Eng. Robot. Res.*, vol. 9, no. 7, pp. 985–991, 2020.
[16] A. Sansudin, "Design and fabrication of a drop-weight impact testing machine for structural materials," *J. Mater. Eng. Perform.*, vol. 29, no. 8, pp. 5121–5128, 2020.
[17] L. Wang and Q. Zhang, "Development of a hydraulic impact testing system for simulation of rock burst conditions," *Int. J. Rock Mech. Min. Sci.*, vol. 134, p. 104112, 2020.
[18] ASTM International, *Standard Test Method for Instrumented Impact Testing (ASTM E2298)*, West Conshohocken, PA, USA, 2018.
[19] R. Saluja, H. Singh, and P. Sharma, "Impact strength evaluation of MIG welded mild steel joints," *Mater. Today Proc.*, vol. 26, pp. 2247–2252, 2020.
[20] R. Appusamy, S. Kumar, and V. Rajesh, "Impact behaviour of natural fibre reinforced polymer composites," *J. Reinf. Plast. Compos.*, vol. 40, no. 5–6, pp. 212–221, 2021.
[21] M. Tekinal and R. Jaya, "Relationship between strain energy and absorbed impact energy using instrumented Charpy testing," *Eng. Fract. Mech.*, vol. 245, p. 107116, 2021.
[22] N. Gupta and R. Kumar, "Design and performance analysis of semi-automated material testing systems," *Int. J. Adv. Manuf. Technol.*, vol. 94, no. 1–4, pp. 345–356, 2018.

Received: 18/03/2026; Revised: 24/03/2026; Accepted: 26/03/2026; Published: 13/04/2026